

# Seismic collapse assessment of non-deteriorating frames with irregular structural properties vulnerable to P-delta



**C. Jäger & C. Adam**

*Department of Civil Engineering Sciences, University of Innsbruck, Austria*

## **SUMMARY:**

In this paper the seismic collapse capacity of multi-story moment resisting frame structures with stiffness and/or strength discontinuities is assessed. The considered structures with non-deteriorating element behaviour are vulnerable to the P-delta effect. The impact of various structural parameters on earthquake induced global collapse is discussed. In particular, it is evaluated, whether the recently developed collapse capacity spectrum methodology may be applied to structures with irregular stiffness and/or strength distribution. Additionally, three alternative modelling strategies for the columns and beams are evaluated. In several example problems the results of the collapse capacity spectrum methodology are set in contrast with outcomes of Incremental Dynamic Analyses.

*Keywords: Dynamic instability; Far-field ground motions; Frame modelling strategies; Structural discontinuity*

## **1. INTRODUCTION**

Building collapse prevention under catastrophic seismic events is one of the primary goals of earthquake engineering. In the most general approach computer time history analysis tools are used to predict collapse of mechanical models, which should represent sufficiently accurate the real building, and in particular, its (inelastic) behaviour under severe earthquake excitation. The disadvantage of this approach is the computational effort needed for e.g. Incremental Dynamic Analyses (IDAs). In particular, in an early stage of the design process computer time is sparsely available, and therefore, it is desirable to have simplified procedures available to assess the collapse capacity fast but sufficiently accurate.

An excellent overview on the state-of-the-art in seismic collapse prediction and simplified approaches provides Villaverde (2007). Simplified procedures are based on various approximations, such as equivalent single-degree-of-freedom (ESDOF) systems and/or the application of nonlinear static (pushover) analyses. In a recently proposed collapse assessment procedure Shafei et al. (2011) combine these methods to assess moment-resisting frame and shear wall structures. Thereby, the global pushover curve is approximated by a trilinear curve, and in combination with structural parameters a closed-form equation is used to estimate the median collapse capacity and the dispersion from aleatory uncertainties.

In this paper the emphasis is on P-delta induced collapse. A recently developed simplified procedure (Adam and Jäger, accepted for publication) for the assessment of the collapse capacity of non-deteriorating moment resisting frame structures vulnerable to the destabilizing effects of gravity loads is summarized. This procedure is based on an ESDOF system with parameters derived from global pushover curves. In contrast to the procedure of Shafei et al. (2011) in this approach bilinear approximations of pushover curves with and without gravity loads are used, and the collapse capacity is determined in combination with collapse capacity spectra. In the present study emphasis is on structures with discontinuities in strength and stiffness.

## 2. COLLAPSE CAPACITY

### 2.1. Definition

The maximum ground motion intensity, at which a given structural system still maintains dynamic stability, is referred to as seismic collapse capacity. Different ground motions lead to different collapse capacities because of the record-to-record variability (Krawinkler et al. 2009). For the present study collapse capacity  $CC_i$  is defined as:

$$CC_i = \frac{S_a(T = T_1, \zeta = 0.05)}{g\gamma} \Bigg|_{\substack{\text{ith ground motion} \\ \text{collapse}}} \quad (2.1)$$

$S_a$  is the normalized 5% damped spectral acceleration at the fundamental structural period  $T_1$  of the considered ground motion record identified by subscript  $i$ .  $g$  is the acceleration of gravity, and  $\gamma$  denotes the base shear coefficient, defined as the ratio of the yielding base shear  $V_y$  to the total weight  $W$  of the structure,  $\gamma = V_y/W$ . Most generally, the computationally IDA procedure (Vamvatsikos and Cornell 2002) is used to determine  $CC_i$ . To capture the record-to-record uncertainties the IDA procedure is not only applied for the  $i$ th ground motion but for a set of representative ground motions, and subsequently the collapse capacities are statistically evaluated. In the present study, 44 ordinary ground motions described in the ATC 63 report are used (FEMA P-695 2009). Sorting of the collapse capacities  $CC_i$  ( $i = 1, \dots, 44$ ) in increasing order yields the associated collapse fragility curve, which describes the probability of collapse for a given ground motion intensity. Ibarra and Krawinkler (2005) have shown that the collapse capacities are distributed log-normally, and thus, only median, 16th percentile and 84th percentile value are necessary to fit a suitable analytical curve to the data points.

### 2.2. Collapse Capacity Spectrum Methodology

The authors have recently presented a fast and yet accurate methodology to predict the collapse capacity of planar regular non-deteriorating moment resisting frame structures vulnerable to P-delta induced structural collapse (Adam and Jäger 2011; Adam and Jäger, accepted for publication), which can be used alternatively to the IDA procedure. The methodology avoids computationally expensive time history analyses. Instead, ESDOF systems based on global pushover curves of the actual structure with and without P-delta effect, in combination with simple charts, referred to as collapse capacity spectra, are used to predict the global collapse capacity. Subsequently, the key points of this procedure are summarized (Adam and Jäger, accepted for publication).

- Based on a first mode horizontal load pattern derive global pushover curve of the considered multi-degree-of-freedom (MDOF) structure with applied gravity loads. If the post-yield stiffness is negative, derive also the global pushover curve without considering gravity loads. Determine the global collapse capacity as subsequently described.
- Perform a bilinear approximation of the pushover curves and identify the global hardening ratio  $\alpha_S$ , and the elastic and inelastic stability coefficient  $\theta_e$  and  $\theta_i$ , respectively, compare with Fig. 2.1(a).
- Derive from  $\alpha_S$ ,  $\theta_e$ , and  $\theta_i$  an auxiliary unique stability coefficient  $\theta_a$  (Adam and Jäger 2011),

$$\theta_a = \frac{\theta_i - \theta_e \alpha_S}{1 - \theta_e + \theta_i - \alpha_S} \quad (2.2)$$

and determine the negative post-yield stiffness ratio  $\theta_a - \alpha_S$ .

- Select a shape vector  $\phi$  for the displacements of the MDOF system with  $N$  stories affine to the fundamental mode to transform the structure into an ESDOF system, and derive the period  $T_a$  of the ESDOF system (Adam and Jäger 2011),

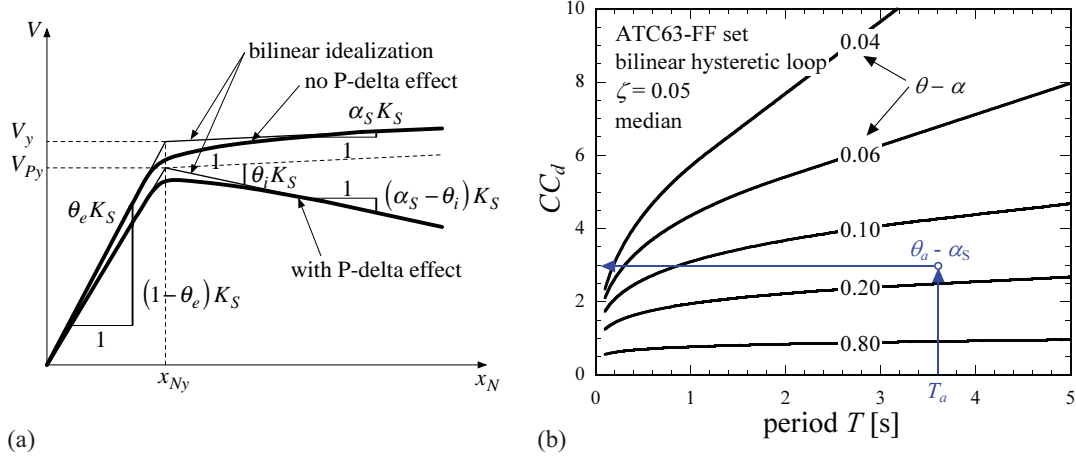


**Figure 2.1.** (a) Pushover curves with and without P-delta of a frame structure and their bilinear approximations. (b) Median collapse capacity spectra (Adam and Jäger 2012)

$$T_a = 2\pi \sqrt{\frac{1 - \alpha_S}{1 - \theta_e + \theta_i - \alpha_S}} \sqrt{\frac{x_{Ny}}{V_y}} \sqrt{\sum_{i=1}^N \phi_i m_i} \quad (2.3)$$

The roof displacement at onset of yielding  $x_{Ny}$  and the corresponding base shear  $V_y$  can be read from the pushover curve without considering gravity loads, compare with Fig. 2.1(a).  $\phi_i$  is the  $i$ th component of  $\boldsymbol{\phi}$ , and  $m_i$  denotes the  $i$ th story mass.

- Consult the appropriate collapse capacity spectrum with respect to the underlying ground motion set, viscous damping  $\zeta$ , hysteretic loop, and the negative post-yield stiffness  $\theta_a - \alpha_S$ , and read at the period  $T_a$  the median collapse capacity  $CC_d$  as shown in Fig. 2.1(b). Analytical relations for  $CC_d$  can be found in Adam and Jäger (2012).
- Transform  $CC_d$  into the domain of the ESDOF system (Adam and Jäger, accepted for publication):

$$CC_{ESDOF} = \frac{CC_d}{\lambda_{MDOF}}, \quad \lambda_{MDOF} = \left( \sum_{i=1}^N \phi_i m_i \right)^2 / \left( \sum_{i=1}^N m_i \sum_{i=1}^N \phi_i^2 m_i \right) \quad (2.4)$$

This outcome is an estimate of the actual median collapse capacity,  $CC_{MDOF} \approx CC_{ESDOF} \cdot \lambda_{MDOF}$  is the transformation coefficient and results from the transformation of the MDOF structure into the ESDOF system.

- Determine the 16th percentile and 84th percentile collapse capacities  $CC_{ESDOF}^{p16}$  and  $CC_{ESDOF}^{p84}$  utilizing relations specified in Adam and Jäger (2012) and determine the collapse fragility curve under the assumption of a log-normal distribution (Ibarra and Krawinkler 2005).

### 3. CONSIDERED BASE-CASE FRAME STRUCTURE

In the present study generic moment resisting frame structures are considered. These 18-story single-bay frames have a uniform story height  $h$ , and uniform lumped masses  $m_s/2$  are assigned to each corner node, as shown in Fig. 3.1(a). In the model the columns are elastic, and the beams rigid, both equipped with bilinear hysteretic springs at the ends, compare with Fig. 3.1(b). The springs have a hardening coefficient  $\alpha = 0.03$ . Justification of this choice is given in chapter 4.1, where different modelling assumptions are evaluated. In the base-case frame the strength of the springs is tuned to obtain in a pushover analysis simultaneous onset of yielding at all springs under a first mode horizontal load pattern. For each story the second moment of area of the columns and the beam is equal. The  $i$ th story stiffness  $K_i$  is given by the relation

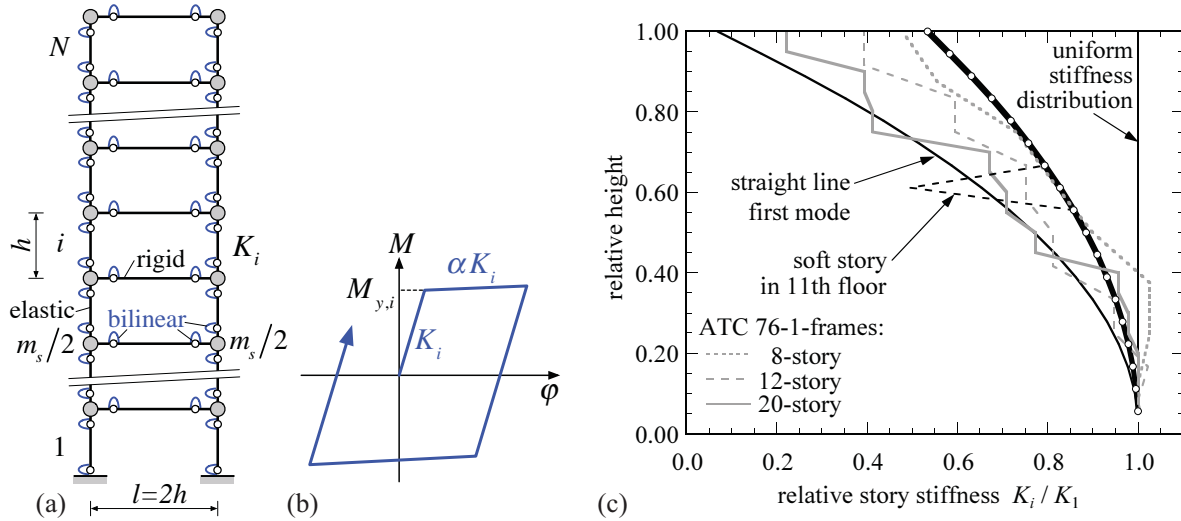


**Figure 3.1.** (a) Generic frame model. (b) Bilinear hysteretic spring behaviour. (c) Story stiffness distribution of generic frame structures and real frames according to ATC 76-1 report (ATC 76-1 2010)

$$K_i = K_1 \left[ 1 - 0.468 \left( \frac{i}{N} \right)^2 \right] \quad (3.1)$$

where  $K_1$  is the stiffness of first story, and  $N$  the number of all stories (here  $N = 18$ ). The absolute stiffness is chosen to obtain a fundamental period of  $T_1 = 3.60$  s. In Fig. 3.1(c) a black bold solid line depicts the stiffness distribution according to this relation. This figure also shows in grey lines the distribution of the story stiffness of real 8, 12, and 20 story moment resisting frame structures designed according to ATC 76-1 report (ATC 76-1 2010). It is evident that relation (3.1) represents adequately the story stiffness distribution of real frames. Note that the relative story stiffness resulting in a straight-line first mode is smaller than the one described by Eqn. (3.1). The relative stiffness for a frame with uniform stiffness distribution is for all stories one. These limit cases are depicted in Fig. 3.1(c) by thin solid black lines. Each frame corner is subjected to the gravity load  $m_s g / 2$ . Rayleigh damping of 5% is assigned to the fundamental mode and that mode, at which the sum of the modal masses exceeds 95% of the total mass. To this base-case frame in selected stories stiffness and/or strength discontinuities are assigned to study their effect on the collapse capacity and its prediction.

## 4. RESULTS

All results presented hereinafter have been calculated using the software framework OpenSees (McKenna et al. 2004) for both Incremental Dynamic Analyses and pushover analyses, respectively.

### 4.1. Frame Modelling Strategies

At first the impact of structural modelling on the collapse capacity and its prediction using the collapse capacity spectra methodology is studied. Three different basic beam/column element models are evaluated. In Fig. 4.1 for each considered basic element the model ID, the symbolic element representation, the moment-rotation-relationship of the element, and the moment-rotation-relationship of the rotational springs at the ends of each element are depicted. The models exhibit properties as described below.

- Model M1 is a linear elastic element. In the study it is used only for columns in a structure perfectly designed according to the strong column–weak beam concept. When using this model for the columns, at the base a rotational spring must be provided, because otherwise no collapse mechanism can occur.

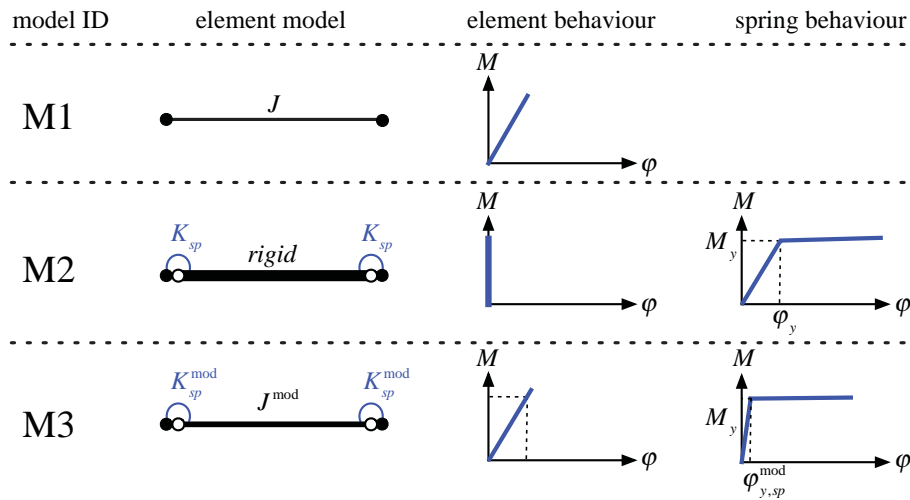


**Figure 4.1.** Modelling strategies for beam and column elements. Overview

- In model M2 all elastic and inelastic properties of the element are assigned to the rotational springs at the both ends of the element, whereas the element itself is considered to be rigid. This model may capture the development of plastic hinges. A disadvantage of this model is that the spring stiffness must be defined a priori, which is a constant regardless of the (changing) moment gradient in the element. For details see Ibarra (2003).
- To avoid this drawback Ibarra and Krawinkler (2005) suggest to keep the beam/column element elastic, and to add rotational springs at the ends, whose rotational stiffness is 10 times stiffer than the rotational stiffness of the elastic beam element. In model M3 two elastic elements are connected in series, and thus, the properties of the parameters can be calibrated according to the “real” behaviour.

Subsequently, eight base-case frame structures are analyzed, using different element models for the beams and/or columns in an effort to evaluate all possible and meaningful combinations of the three basic models. Additionally, for the beams a distributed plasticity model (denoted as d.p.) is utilized, with 10 integration points along the element axis and a moment-rotation-relationship as shown in Fig. 3.1(b). The considered column/beam element combinations are M1/M2, M1/M3, M2/M2, M2/M3, M3/M2, M3/M3, M2/d.p., and M3/d.p. Fig. 4.2(a) shows for all considered structures median IDA curves based on the ATC63-FF record set. One can observe that for small intensities and moderate plastic deformations all models predict the same median peak displacement of the roof. All frames composed of column-models M2 and M3 collapse at an intensity of approximately  $S_a(T=T_1, \zeta=0.05)/(g\gamma) = 3.0$ , because plastic hinges in the columns lead to a plastic mechanism. The frames designed according to the strong column-weak beam concept (model M1 for the columns) exhibit a pronounced larger collapse capacity, emphasizing the importance of a large ratio of column to beam strength. For comparison, also IDA curves for frames with beams composed of distributed plasticity models are shown. It can be concluded that both models M2 and M3 with appropriate springs can be used for the beams without influencing substantially the collapse capacity predictions.

In Fig. 4.3(a) the corresponding first mode pushover curves considering gravity loads are displayed. Frames designed according to the strong column-weak beam concept exhibit a favourable post-yielding behaviour. The pushover curves of these frames exhibit a constant negative slope in the inelastic range of deformation, because no plastic hinges develop in the columns. The pushover curves depicted by red solid lines correspond to structures with columns composed of element model M2. The results of Fig. 4.3(a) reveal that this model option overestimates the post-yield stiffness, because in the stiffness matrix of element M2 no translational stiffness terms do exist. That is why the higher modes of models based on column elements M2 do not coincide with the ones of the corresponding unlimited elastic model. For example, the period of the 5th mode is about 15% lower than the actual

one of the elastic model. However, when for the columns element M3 is used, the actual structural behaviour is reproduced. Thus, in the studies of chapter 4.2 element M3 is utilized for the columns, while for simplicity the beams consist of element M2 without introducing significant errors.

Fig. 4.2(b) depicts for the considered structures the “exact” median collapse capacities obtained from IDAs with black bars, the corresponding estimated values  $CC_d$  based on the collapse capacity spectrum methodology are given in grey. It is readily seen that for frames composed of the unlimited elastic column model M1 the collapse capacity spectrum methodology overestimates the “real” collapse capacity. In contrast, in all other examples, where columns may exhibit plastic hinges, the collapse capacity spectrum methodology underpredicts the collapse capacity. However, for all considered structures the maximum difference is 16% compared to the outcomes from IDAs.

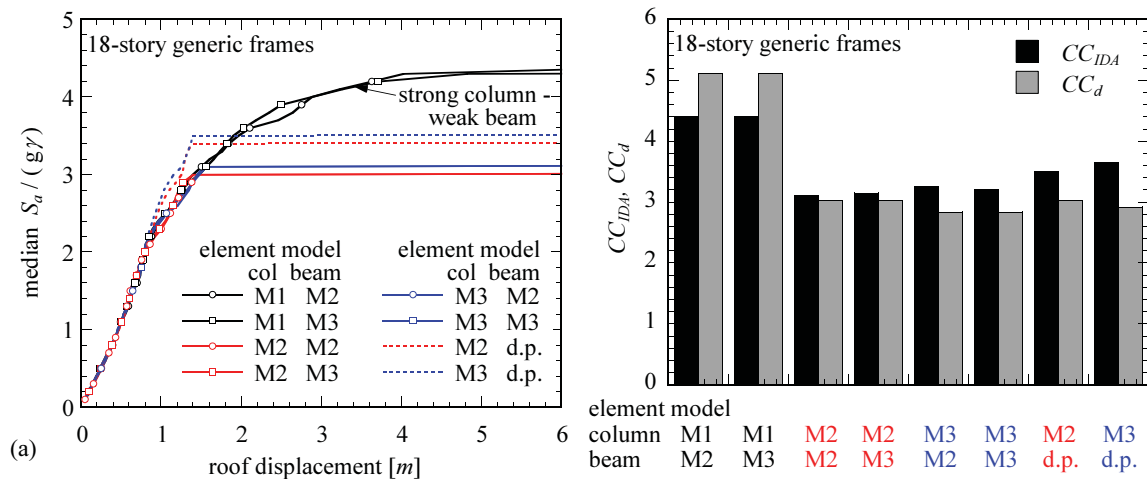


**Figure 4.2.** (a) Incremental dynamic analysis of generic frames with different element modelling. (b) Comparison of median collapse capacities based on IDAs and on the collapse capacity spectrum methodology

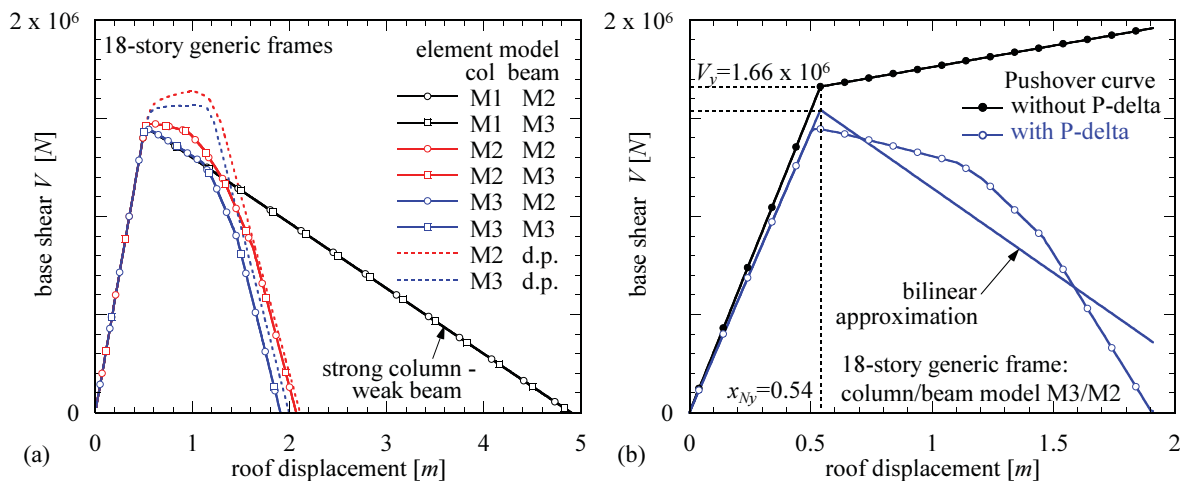


**Figure 4.3.** (a) Global first mode pushover curves with P-delta effect for frames with different element models. (b) Bilinearization of one pushover curve

The collapse capacity spectrum methodology is based on bilinear approximations of the pushover curves. In the considered examples this bilinearization is straight forward for the frames designed according to the strong column-weak beam concept. However, the pushover curves of the frames with plastic hinges in the columns do not exhibit a uniform slope in the post-yield range of deformation, as

can be seen from Fig. 4.3(a). Exemplarily, in Fig. 4.3(b) the global pushover curves with and without gravity loads of the 18-story frame composed of column/beam models M3/M2 are depicted. The sharp kink in the pushover curve without gravity loads can be led back to particular tuning of the spring strengths as described in chapter 3.1. For this example the roof yield displacement is  $x_{Ny} = 0.54$  m, and the corresponding base shear is  $V_y = 1.66 \times 10^6$ . Additionally, the bilinearized pushover curve is shown by a solid blue line, using the method of least squares to determine the slope of the line of best fit.

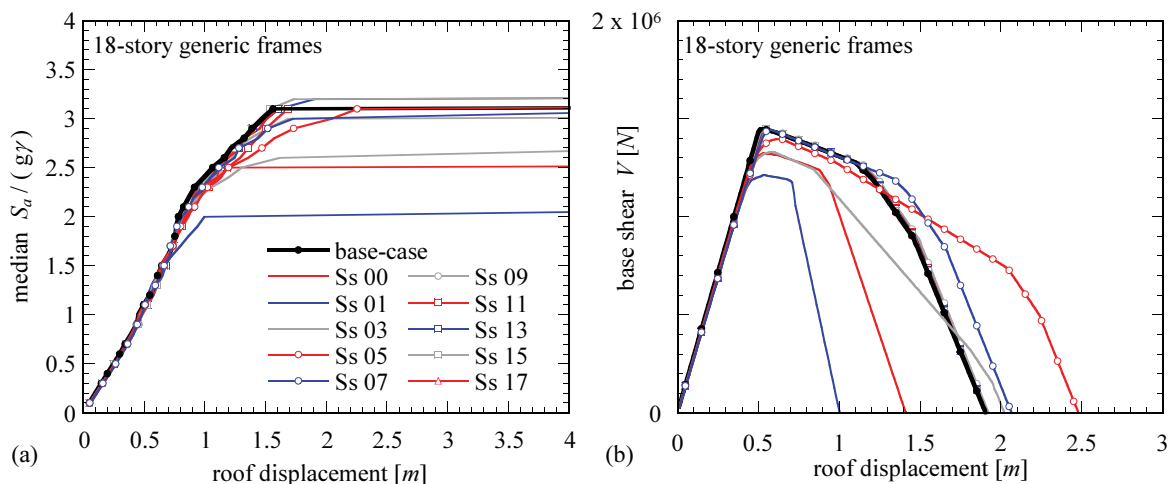
#### 4.2. Effect of Stiffness and Strength Discontinuities

The fundamental assumption of the collapse capacity spectrum methodology is that the dynamic behaviour of the actual MDOF structure can be represented by an ESDOF system. This assumption is questionable, if the structure exhibits irregularities and discontinuities in story strength and/or story stiffness. Therefore, subsequently the impact of soft stories is evaluated. According to Chen and Lui (2005) a “soft story” does exist, if

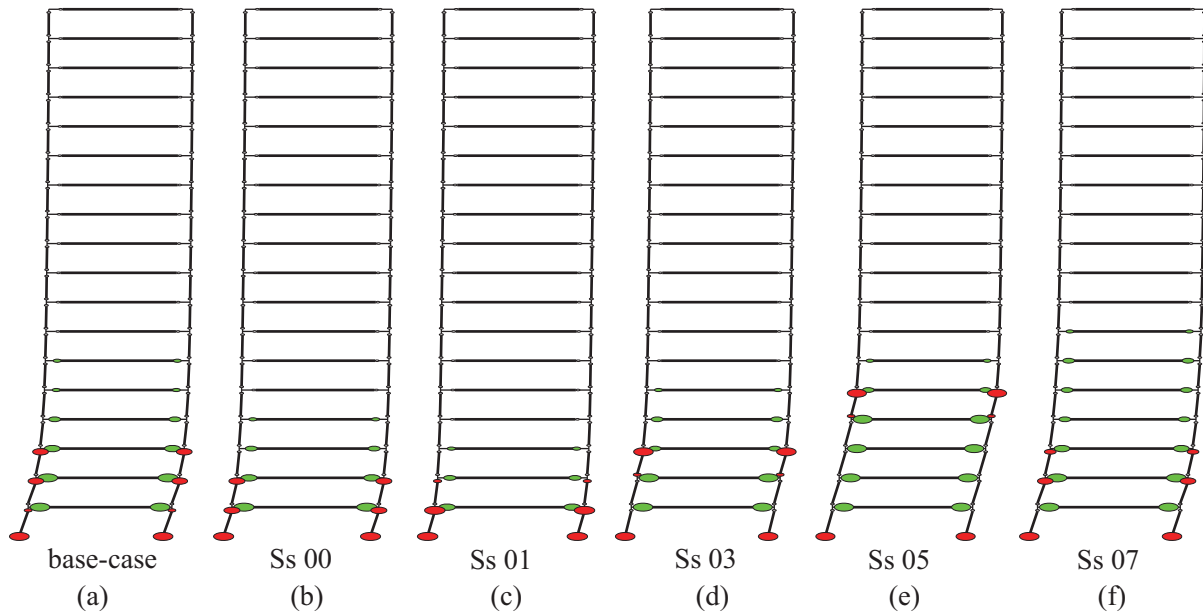
- the lateral stiffness of a story is 70% or less than that in the story above, or
- less than 80% of the average stiffness of the three stories above.

In the following, the collapse capacity of altogether thirty different frame structures is evaluated. The considered frames exhibit a stiffness discontinuity, a strength discontinuity, or a combined stiffness/strength discontinuity. The discontinuity is 60% of the initial stiffness and/or strength of the corresponding base-case frame, and it is imposed to the first, third, fifth, ..., seventeenth floor, respectively. Accordingly, also the base springs are modified (denoted by “00”). As an example, Fig. 3.1(c) shows the stiffness distribution of a frame with a soft story in the 11th floor.

Fig. 4.4(a) shows median IDA curves of various 18-story generic frame structures with combined stiffness and strength discontinuities. In the legend of this figure the story number indicates the affected story. For comparison, a solid black line depicts the median IDA curve of the original base-case frame with continuous stiffness and strength distribution. It can be seen that frames with a structural discontinuity at the base, first floor, and third floor exhibit a smaller median collapse capacity than the original undisturbed frame. The frame with a soft first story has the smallest median collapse capacity of about  $CC_{IDA} = 2.0$  compared to  $CC_{IDA} = 3.0$  of the original frame. In all other frame structures the discontinuity does not reduce significantly the median collapse capacity, because P-delta affects primarily the lower stories, where the gravity loads are largest.



**Figure 4.4.** (a) Median IDA curves of generic frames with combined stiffness/strength discontinuities in different stories. (b) Corresponding global first mode pushover curves with P-delta effect



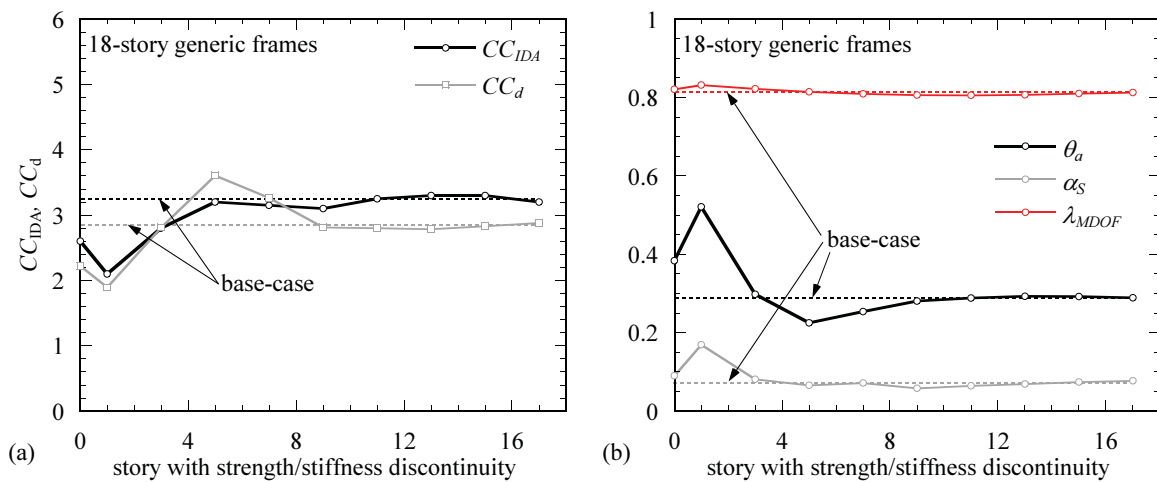
**Figure 4.5.** Deformed first mode pushover profiles of the (a) base-case frame, (b) frame with reduced base spring stiffness and strength, (c) frame with reduced stiffness and strength of the first, (d) third, (e) fifth, and (f) seventh floor

Fig. 4.4(b) shows the corresponding global pushover curves, which are the basis of the collapse capacity spectrum methodology. The pushover curve of the frame with a first story soft floor exhibits the lowest global strength and poorest global ductile behaviour. The higher the structural discontinuity, the larger the global strength, and the better the ductile behaviour. If the soft story is in the fifth floor, the global structural behaviour is superior, also compared to the original base-case frame. Stiffness and strength discontinuities above the seventh floor do not affect the global pushover curve considerably. To support and justify these observations in Fig. 4.5 the corresponding deformed shapes of the frames at a base shear of 800000 N (in the post-elastic domain) are depicted. Fig. 4.5(a) shows the displacement profile of the original undisturbed frame, Figs 4.5(b)-4.5(f) represent the profiles of frames with a stiffness/strength discontinuity at the base (b), the first (c), third (d), fifth (e), and seventh (f) floor. Red and green circles identify a plastic hinge, the size of these circles depends on the actual ductility. In the base-case frame the plastic rotations are concentrated in the lower stories. The plastic rotations are amplified in frames with a discontinuity in the lower levels. If the structural irregularity is located in the fifth floor, a partial mechanism evolves in first five floors, with more or less uniform plastic rotations at the beam ends. No plastic hinges occur in the columns until the fifth floor, and thus, energy is dissipated more uniformly in these lowest stories compared to the frames of Figs 4.5(a)-4.5(d). As shown in Fig. 4.5(f), a stiffness and strength reduction of 40% in the seventh floor does not lead to the formation of such a favourable mechanism as in the frame with soft fifth story. Here, the mechanism is similar as in the base-case frame. Thus, the global pushover curves of the frames with structural discontinuities in the higher levels coincide with the curves of the base-case structure. It is emphasized that the presented results strongly depend on the frame geometry and on the actual strength and/or stiffness reduction.

In Fig. 4.6(a) the median collapse capacity of the considered frames with both stiffness and strength discontinuity is plotted against the location of the discontinuity. The “exact” median collapse capacities (from IDA procedure) are displayed in black, while the estimated counterparts based on the collapse capacity spectrum methodology are displayed in grey. In most cases the simplified collapse capacity prediction is conservative. It is striking that the difference between the exact and estimated collapse capacity is almost constant. However, for the frame with discontinuity in the fifth floor, the collapse capacity spectrum methodology yields a slightly unconservative collapse prediction. This is the effect of the favourable local mechanism, which leads to a smaller auxiliary stability coefficient  $\theta_a$  compared to the other frames, see Fig. 4.6(b). Therefore, when applying the collapse capacity

spectrum methodology it is suggested to check additionally the deformed profile of the first mode pushover analysis whether it is P-delta characteristic. I.e., the plastic hinges are located in the lower stories, and no partial plastic mechanism develops, as in the example of Fig. 4.5(e). P-delta characteristic deformed shapes are shown in Figs 4.5(a), 4.5(b) and 4.6(c).

In Fig. 4.7(a) median collapse capacities (black lines) from IDAs and their estimated counterparts (grey lines) based on the collapse capacity spectrum methodologies are shown for the base-case frame and for frames with structural discontinuities in the specified story. Thereby, frame structures are considered, where either the stiffness or the strength is reduced in selected stories, additionally to structures with a combined reduction of strength and stiffness. The results reveal that a strength reduction in the lower stories is more crucial than a stiffness reduction. A discontinuity in the upper stories is less crucial, and the median collapse capacities are close to ones of the original undisturbed base-case frame.



**Figure 4.6.** (a) Comparison of median collapse capacities based on IDAs and on the collapse capacity spectrum methodology for the frame subset with both stiffness and strength discontinuities. (b) Significant ESDOF parameters for the collapse capacity spectrum methodology

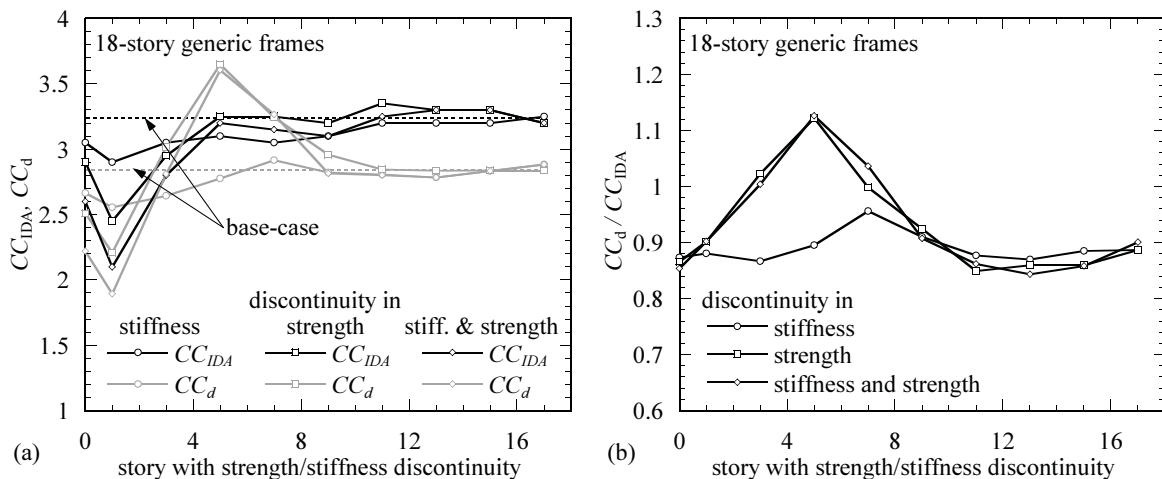


**Figure 4.7.** (a) Comparison of median collapse capacity prediction based on IDAs with results from the collapse capacity spectrum methodology. (b) Ratios of these predictions

In Fig. 4.7(b) the ratio of the simplified determined median collapse capacity to the median collapse capacity based on IDAs is plotted against the location of the discontinuity. It can be seen that for the structure with strength discontinuity in the fifth floor the collapse capacity spectrum methodology overestimates the median collapse capacity by about 12%. For most of the other structures the simplified method underpredicts collapse by about 10%.

## 5. SUMMARY

It could be shown that the collapse capacity spectrum methodology can be applied also for planar frame structures that exhibit distinct irregularities in story stiffness and/or story strength. Thus, the assumption that the pushover curve represents the mechanism, which may develop in the P-delta vulnerable structure during a severe earthquake, is confirmed. Furthermore, it was shown that a structural discontinuity in the upper floors does not affect significantly the global collapse capacity. The results of this study confirm that *rigid* elements equipped with elastic-plastic rotational springs at the ends model sufficiently accurate the beam behaviour of the considered P-delta sensitive frame structures. In contrast, in the mechanical model the columns should be composed of *elastic* elements with elastic-plastic rotational springs at the ends to reflect appropriately the inelastic mechanism, which may lead to global collapse.

## ACKNOWLEDGEMENT

The presented investigations of the first author were partially funded by the Tyrolean Science Fund (TWF). This financial support is gratefully acknowledged.

## REFERENCES

- Adam, C. and Jäger, C. (2011). Seismic induced global collapse of non-deteriorating frame structures. In Papadrakakis, M., Fragiadakis, M. & Lagaros, N.D. (eds.), *Computational Methods in Earthquake Engineering*. Dordrecht, Springer, 21-40.
- Adam, C. and Jäger, C. (2012). Seismic collapse capacity of basic inelastic structures vulnerable to the P-delta effect. *Earthquake Engineering and Structural Dynamics* **41**, 775-793.
- Adam, C. and Jäger, C. (accepted for publication). Simplified collapse capacity assessment of earthquake excited regular frame structures vulnerable to P-delta. *Engineering Structures*
- ATC 76-1 (2010). Evaluation of the FEMA P-695 Methodology for Quantification of Building Seismic Performance Factors. 100% draft. *National Institute of Standards and Technology*.
- Chen, W.F. and Lui, E.M. (2005). *Earthquake Engineering for Structural Design*. CRC Press.
- FEMA P-695 (2009). Quantification of Building Seismic Performance Factors. Federal Emergency Management Agency, Washington D.C.
- Ibarra, L.F. (2003). Global collapse of frame structures under seismic excitations. PhD Thesis. Stanford University.
- Ibarra, L.F. and Krawinkler, H. (2005). Global collapse of frame structures under seismic excitations. *Report No. PEER 2005/06*. Berkeley, CA: Pacific Earthquake Engineering Research Center, University of California.
- Krawinkler, H., Zareian, F., Lignos, D.G. and Ibarra, L.F. (2009). Prediction of collapse of structures under earthquake excitations. In Papadrakakis, M., Lagaros, N.D. and Fragiadakis M. (eds), *2nd International Conference on Computational Methods in Structural Dynamics and Earthquake Engineering (COMPDYN 2009)*. CD-ROM paper, paper no. CD449.
- McKenna, F., Fenves, G.L. and Scott, M.H. (2004). OpenSees: Open system for earthquake engineering simulation. Pacific Earthquake Engineering Research Center, University of California, Berkeley, California. Available at <http://opensees.berkeley.edu>
- Shafei, B., Zareian, F. and Lignos, D.G. (2011). A simplified method for collapse capacity assessment of moment-resisting frame and shear wall structural systems. *Engineering Structures* **33**, 1107-1116.
- Vamvatsikos, D. and Cornell, C.A. (2002). Incremental dynamic analysis. *Earthquake Engineering and Structural Dynamics* **31**, 491-514.
- Villaverde, R. (2007). Methods to assess the seismic collapse capacity of building structures: State of the art. *Journal of Structural Engineering* **133**, 57-66.